Measurement of the (n, 2n) reaction cross-sections of iodine and cesium induced by D-T neutrons with covariance analysis*

Changlin Lan (兰长林)[1†] Yuxing Niu (牛玉鑫)[1,2] Yuting Wei (魏玉婷)[1‡] Fangxiao Lu (陆芳潇)[1]
Xianlin Yang (杨宪林)[1] Ruirui Xu (续瑞瑞)[3] Yue Zhang (张玥)[3] Yujie Ge (葛裕杰)[1]
Jiahao Wang (王家豪)[1] Gong Jiang (姜功)[1]

[1]School of Nuclear Science and Technology, Lanzhou University, Lanzhou 730000, China
[2]China National Nuclear Corporation, Beijing 100045, China
[3]Key Laboratory of Nuclear Data, China Institute of Atomic Energy, Beijing 102413, China

Abstract: The cross-sections of the ^{127}I (n, 2n) ^{126}I and ^{133}Cs (n, 2n) ^{132}Cs reactions at neutron energies of 13.83 ± 0.05, 14.33 ± 0.10, and 14.79 ± 0.10 MeV were measured relative to the ^{93}Nb (n, 2n) ^{92m}Nb reaction using the activation technique in combination with off-line γ-ray spectrometry. A neutron beam was generated from the T (d, n) ^{4}He reaction using the K-400 neutron generator at the China Academy of Engineering Physics. Considering the correlations between different attributes, detailed uncertainty propagation was performed using covariance analysis, and the cross-sections were reported with their uncertainties and correlation matrix. The uncertainty of the measurement cross-sections ranged from 4.84 to 5.90%, which is lower than previous experimental data. Furthermore, the theoretical excitation functions of the ^{127}I (n, 2n) ^{126}I and ^{133}Cs (n, 2n) ^{132}Cs reactions were calculated using the TALYS-1.95 and EMPIRE-3.2.3 codes. Then, the experimentally determined cross-sections were analyzed by comparing them with literature data available in the EXFOR database and evaluated nuclear data in the ENDF/B-VIII.0, JEFF-3.3, JENDL-5, BROND-3.1, CENDL-3.2, and TENDL-2021 databases. Compared with the values previously reported in the 13.8-14.8 MeV energy region, the precision of the results obtained in this study was greatly improved. The current experimental results with thorough uncertainties and covariance information are critical for verifying the reliability of the theoretical model and improving the quality of the nuclear database.

Keywords: ^{127}I (n, 2n) ^{126}I, ^{133}Cs (n, 2n) ^{132}Cs, cross-section, neutron activation, covariance analysis, excitation function

DOI: 10.1088/1674-1137/ace313

I. INTRODUCTION

Accurate measurement of neutron-induced cross-sections is of significant importance in the study of nuclear reaction mechanisms and reactor technology. Such data also play a key role in nuclear transmutation calculations and the evaluation of nuclear models [1]. As neutron breeder materials, the cross-sections of iodine and cesium induced by neutrons in the energy range of approximately 13 to 15 MeV are vital for the construction of fusion reactors and fourth generation fast reactors, as well as the measurement of neutron energy spectra using the activation method. The activation cross-sections of neutron-induced iodine and cesium reactions have been measured by several groups; however, most were obtained 30 years ago, and the data are highly scattered [2−21]. The majority of ^{127}I (n, 2n) ^{126}I cross-section measurements were made before 1990, and only data measured by Gandhi were taken after 2000 [2−15, 22]. The deviation of these experimental measurements almost exceed 100%, and the uncertainty of most experimental sections is greater than 10%. As an example, the cross sections of the ^{27}I (n, 2n) ^{126}I reaction measured by Maslov *et al*. and Santry *et al*. are significantly higher than other literature data [5, 6]. The latest cross-section of the ^{133}Cs (n, 2n) ^{132}Cs reaction was obtained almost 30 years ago, and most studies only measured one or two energy points [6−8, 16−21]. Although Bormann measured for a wide range of energies, the data were far fewer than the cross-sections measured by other studies and the excitation functions of the evaluation database [13, 17]. Therefore, re-measuring is necessary to obtain more precise cross-

Received 2 May 2023; Accepted 28 June 2023; Published online 29 June 2023
* Supported by the Key Laboratory of Nuclear Data Foundation (JCKY2022201C151), and the National Natural Science Foundation of China (11975113).
† E-mail: lanchl@lzu.edu.cn
‡ E-mail: weiyt2021@lzu.edu.cn

sections of ^{127}I (*n, 2n*) ^{126}I and ^{133}Cs (*n, 2n*) ^{132}Cs around the 14 MeV energy region.

In addition, the uncertainty accompanying the activation cross-section is essential in determining a reasonable margin, which contributes to both safety and economy in nuclear applications [23, 24]. If several data points of the activation cross-sections are involved in determining the quantity of interest, the correlation (covariance) among the data points must also be considered to avoid overestimating or underestimating the uncertainty in the quantity of interest [25]. Therefore, modern evaluation reports attempt to provide not only the best estimate of the cross-section but also the uncertainty and covariance describing the correlation among the cross-sections. However, in most previous data, details are not reported on error propagation and correlations among the different attributes. Considering the above facts, new experimental cross-sections with covariance analysis are needed to verify the reliability and improve the accuracy of these evaluated nuclear data and theoretical models.

In this study, the cross-sections of the ^{127}I (*n, 2n*) ^{126}I and ^{133}Cs (*n, 2n*) ^{132}Cs reactions at neutron energies of 13.83 ± 0.05, 14.33 ± 0.10, and 14.79 ± 0.10 MeV were measured via neutron activation in combination with a high purity germanium (HPGe) detector. Then, a detailed covariance analysis was performed to estimate the uncertainty of the cross-sections and the correlation matrix between different reaction cross-sections. The experimental results were compared to existing cross-section data available in the EXFOR database and evaluated data of the ENDF/B-VIII.0, JEFF-3.3, JENDL-5, BROND-3.1, CENDL-3.2, and TENDL-2021 libraries. The excitation function of the nuclear reactions was calculated in the neutron energy range from the threshold to 20 MeV using the nuclear theoretical model programs TALYS-1.95 and EMPIRE-3.2.3. The motivation for performing these theoretical model calculations was to reproduce the best-estimated results compared to the present measured cross sections and existing experimental data reported in the EXFOR database [22].

II. EXPERIMENT DETAILS

The cross-sections of the ^{127}I (*n, 2n*) ^{126}I and ^{133}Cs (*n, 2n*) ^{132}Cs reactions were determined by measuring the characteristic γ-rays emitted from the generated radionuclides. The samples were activated by neutron irradiation, and then the gamma spectrum was obtained by off-line measurements with a low background HPGe detector.

A. Sample

The cesium iodide (CsI) powder of natural isotopic composition (purity 99.99%) was pressed into a pellet (approximately 20.0 mm in diameter, and 1.5 mm in thickness). Monitor foils of natural niobium foils (purity 99.99%, and 0.1 mm in thickness) of the same diameter as the pellet were attached at the front and back of each CsI sample. Three groups of such samples were prepared for irradiation and measurement.

B. Irradiation and neutron energy determined

Irradiation was carried out using the K-400 Intense Neutron Generator at the China Academy of Engineering Physics (CAEP) and lasted approximately 17 h with a yield of approximately 3 to 4×10^{10} n/(4πs). The deuteron ion beam current was 180 μA with of an energy of 250 keV. The solid tritium-titanium (T-Ti) target used in the generator was approximately 2.59 mg/cm^2 thick. A schematic diagram of the sample positions is shown in Fig. 1. The groups of samples were placed at 35°, 75°, and 112° relative to the deuteron beam direction and centered around the T-Ti target at a distance of approximately 4.5 cm. During irradiation, the variation in the neutron yield was monitored by the accompanying α particles to make corrections for the fluctuation of the neutron flux. The neutron energy determined by the *Q* equation was (13.83 ± 0.05) MeV, (14.33 ± 0.10) MeV, and (14.79 ± 0.10) MeV, respectively [26, 27]. The uncertainties in the incident neutron energies given above were the quadratic summation of the uncertainties caused by the energy straggling of the incident deuteron ions on the T-Ti target and the angle divergence from the target to samples [28].

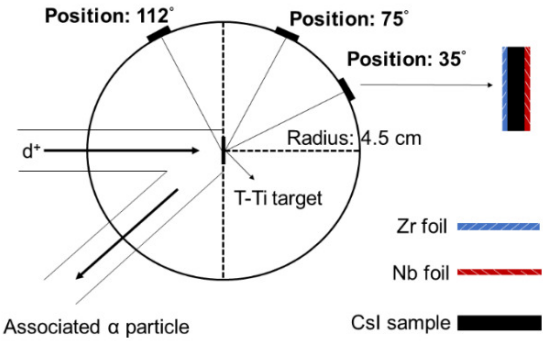

Fig. 1. (color online) Schematic diagram of experimental geometry.

C. Gamma spectroscopic measurements

The γ-rays emitted from the activation sample were measured by continuous off-line measurements with a lead-shielded HPGe detector (ORTEC, USA). The signals were collected by ORTEC MAESTRO software, which provided precise deadtime information. Before measurement, the efficiency of the detector was calibrated using ^{152}Eu standard sources with known activity. The relative efficiency of the detector was 68% compared to the NaI detector, and the energy resolution was 1.82 keV (FWHM) at 1.33 MeV of ^{60}Co. The details of

Table 1. Nuclear decay data and their uncertainties used in this experiment [29–31].

Reaction	Abundance of target isotope (%)	Half-life of product /d	E_γ of product /keV	I_γ of product (%)
^{127}I (n, $2n$) ^{126}I	100	12.930 ± 0.050	388.633	35.600 ± 0.600
^{133}Cs (n, $2n$) ^{132}Cs	100	6.479 ± 0.007	464.466	1.580 ± 0.090
^{93}Nb (n, $2n$) ^{92m}Nb	100	10.150 ± 0.020	934.440	99.150 ± 0.040

the nuclear decay data and their uncertainties used in this experiment are given in Table 1.

III. DATA ANALYSIS

A. Efficiency calibration of the detector with uncertainty

A standard ^{152}Eu point source of known activity was used to calibrate the efficiency of the HPGe detector. Various characteristic γ-rays of ^{152}Eu were measured by placing the source at a distance of approximately 5 cm from the detector [32, 33]. The nine considered characteristic γ-rays of the standard ^{152}Eu source were 121.782 keV, 244.697 keV, 344.279 keV, 411.117 keV, 778.905 keV, 867.380 keV, 1112.067 keV, 1299.142 keV, and 1408.013 keV. The obtained efficiencies for the characteristic γ-ray energies of ^{152}Eu are plotted in Fig. 2. The efficiency calibration curve was fitted to a polynomial function to obtain the most accurate values using the following expression [23–25, 33]:

$$\ln\epsilon = p_1 + p_2(\ln E) + p_3(\ln E)^2 + \cdots + p_m(\ln E)^{m-1}, \quad (1)$$

where p_m is the fitting parameter. The best quality of fit was achieved for $m = 2$, with $x_m^2/(9-m) \approx 1$ [25]. The polynomial function is given as

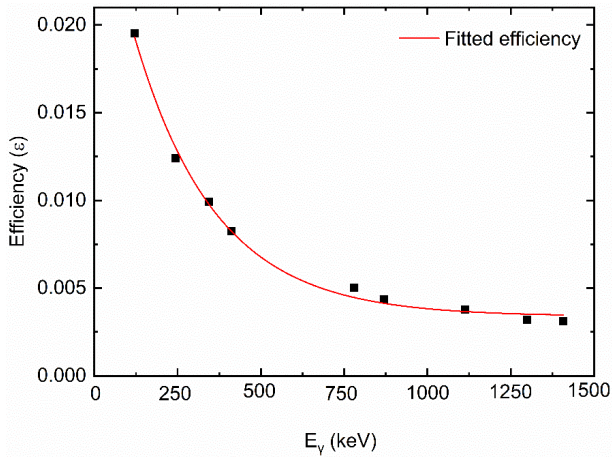

Fig. 2. (color online) Efficiency calibration curve of the HPGe detector for the sample geometry source placed at a distance of 5 cm from the top of the detector.

$$\ln\epsilon = -5.331079 - 0.661669\ln E. \quad (2)$$

By substituting the γ-ray energies in Eq. (2), the efficiencies of the γ-rays emitted from ^{126}I and ^{132}Cs were obtained. The covariance matrix $V_{\epsilon c}$ at the characteristic γ-rays of the reaction products ^{126}I, ^{132}Cs, and ^{92m}Nb was determined by the equation in Refs. [25, 33]. Table 2 presents the detector efficiency estimates corresponding to the characteristic γ-ray energies of the reaction products along with the correlation matrix. The estimated efficiencies were required for further cross-section calculation.

Table 2. Interpolated detector efficiencies of the radionuclide with its correlation matrix.

Type of reaction	Efficiency	Correlation matrix		
^{127}I (n, $2n$) ^{126}I	0.00904 ± 0.00018	1		
^{133}Cs (n, $2n$) ^{132}Cs	0.00804 ± 0.00019	0.99845	1	
^{93}Nb (n, $2n$) ^{92m}Nb	0.00506 ± 0.00018	0.98410	0.99247	1

B. Determination of reaction cross-sections and the corresponding uncertainty

The reaction cross-sections of ^{127}I (n, $2n$) ^{126}I and ^{133}Cs (n, $2n$) ^{132}Cs were determined using the following expression [23, 34]:

$$\sigma_x = \sigma_m \frac{A_x \lambda_x a_m N_m I_{\gamma(m)} \epsilon_m f_m}{A_m \lambda_m a_x N_x I_{\gamma(x)} \epsilon_x f_x} \times \frac{C\mathrm{attn}_x}{C\mathrm{attn}_m}, \quad (3)$$

where σ represents the cross-section, the subscripts m and x represent the monitor reaction and measured reaction, respectively, A is the full energy peak area of the characteristic γ-ray, λ is the decay constant of the product nucleus, a is the abundance of the target nuclei, N is the number of atoms, I_γ summarized in Table 1 is the branching intensity of γ-rays, ϵ is the full-energy peak efficiency, f is the time factor, given by $(1-\mathrm{e}^{-\lambda T})\times(1-\mathrm{e}^{-\lambda t})\mathrm{e}^{-\lambda\Delta t}$, T is the irradiation time, Δt is the cooling time, t is the measurement time, and Cattn is the total correction factor of the counting process, given by $C\mathrm{attn} = F_S * F_C * F_g$ (F_S, F_C, F_g are the self-absorption correction factor, cascade coincidence correction factor,

and geometric correction factor, respectively).

The uncertainty propagation in the measured cross-sections was determined by considering the fractional uncertainty in various attributes, *i.e.*, the timing factor (f_x, f_m), efficiency (ϵ_x, ϵ_m), γ-ray intensity ($I_{\gamma(x)}$, $I_{\gamma(m)}$), isotopic abundance of the nuclei (η), number of atoms (N_x, N_m), γ -ray characteristic peak counts (A_x, A_m), and monitor reaction cross-section (σ_m). The uncertainties in T, t, and Δt were so small that they could not be incorporated into the uncertainty of the final reaction cross-sections. Hence, the uncertainty in the final cross-section of this study was calculated as

$$\delta\sigma_x = \sqrt{\sum_1^4 \delta^2_{(\sigma,E_i)x} + \sum_1^4 \delta^2_{(\sigma,E_j)m} + 2\sum \delta_{(\sigma,E_i)\epsilon_x} \mathrm{Corr}(\epsilon_x,\epsilon_m)\delta_{(\sigma,E_j)\epsilon_m}} \quad (4)$$

C. Covariance analysis

Covariance analysis is a mathematical tool that can help to describe detailed uncertainties with cross-correlation among different measured components. Nuclear data are an experimental quantity with applications including the design of fission and fusion reactors and nuclear medicine [23, 24]. Therefore, it is necessary for measurement experiments that generate these types of quantitative information to perform carefully and report the experimental investigation in detail, including the experimental uncertainties and their covariance matrix. Meanwhile, this detailed information helps the evaluator assess the nuclear data precisely and correctly. In this study, the radioactivity of all irradiated samples was measured with the same detection system, and the same standard reference reaction cross-section was used for calculation. Hence, the detector efficiency and standard cross-section accuracy were the same for all neutron energies, indicating that the neutron energies were correlated with each other. For the calculation of uncertainty in the measured cross-sections and its covariance matrix, the counts of the γ-ray spectra and other parameters with definite uncertainties were also considered.

The fractional uncertainties from all of these parameters and the correlation coefficients between different reaction cross-sections are summarized in Table 3. Based on these fractional uncertainties and correlation coefficients, the results of the measured reaction cross-sections with their uncertainties and correlation matrix are presented in Table 4.

IV. THEORETICAL CALCULATION

The mutual verification between theory and experiment is critical for obtaining reliable and accurate nuclear data. Therefore, theoretical nuclear codes such as EMPIRE and TALYS have been developed as reliable tools to calculate reaction cross sections, including those of photons, neutrons, protons, tritons, deuterons, α-particles, and ^{3}He as projectiles for target nuclei. The excitation functions of the ^{127}I (n, $2n$) ^{126}I and ^{133}Cs (n, $2n$) ^{132}Cs reactions in the neutron energy region from the threshold to 20 MeV were calculated using the TALYS-1.95 and EMPIRE-3.2.3 codes [29, 30]. The calculations were based on different mechanisms of the nuclear reactions, which vary with incident energy. Three major reaction mechanisms, including direct reaction (DI), pre-equilibrium emission (PE), and compound nucleus (CN), are considered in these codes. To estimate the contributions from all such mechanisms, the codes incorporate various nuclear models that use different sets of optical model parameters, level density, and so on. The contributions from all three mechanisms compose the total reaction cross section. The theoretical calculations were performed by employing the optimum combination of input parameters, and their values were obtained for various models and parameters.

A. TALYS-1.95 calculation

TALYS is a nuclear reaction program that can calculate the nuclear reaction cross-sections of photons, neutrons, protons, tritons, deuterons, α-particles, and ^{3}He in the 0.001 –200 MeV energy range and target nuclides with nuclear masses of 12 or heavier. The nuclear reaction models of the optical model, pre-equilibrium reactions, compound reactions, and level densities, are all contained in the TALYS-1.95 code. The distorted wave Born approximation (DWBA) model was used for the direct reaction contribution, and the calculation was performed using ECIS-06 code [35, 36]. The two-component exciton model developed by Kalbach was used to calculate the pre-equilibrium emission contribution, and the compound nucleus contribution was calculated using the Hauser-Feshbach statistical model with width model correction using the Moldauer model [37−39]. To understand the effect of nuclear level density and pre-equilibrium emission on the excitation function of neutron induced reactions, an excitation function was estimated using six different nuclear level density models (default parameters: Idmodel 1) and four pre-equilibrium models (default parameter: preedmode 2) in TALYS-1.95 code.

B. EMPIRE-3.2.3 calculation

In EMPIRE, the description of the compound level density parameter was obtained according to the Gilbert–

Table 3. Fractional uncertainties and correlations in various attributes of the measured reactions.

Reaction	E_n /MeV	Number (x)	A	ε	I_γ	f
	13.83 ± 0.05	1	1.8637E-08	0.2379	0.0239	4.0049E-03
^{127}I (n, 2n) ^{126}I	14.33 ± 0.10	2	2.7367E-08	0.2593	0.0261	4.3847E-03
	14.79 ± 0.10	3	3.2182E-08	0.2669	0.0268	4.5307E-03
	13.83 ± 0.05	4	1.2240E-06	0.2487	0.0376	6.3374E-04
^{133}Cs (n, 2n) ^{132}Cs	14.33 ± 0.10	5	1.7722E-06	0.2749	0.4152	7.1028E-04
	14.79 ± 0.10	6	2.0109E-06	0.3030	0.0458	7.9252E-04
	Cor (1,1)		1	1	1	1
	Cor (1,2)		0	1	0	0
	Cor (1,3)		0	1	0	0
	Cor (1,4)		0	0.9984	0	0
	Cor (1,5)		0	0.9984	0	0
	Cor (1,6)		0	0.9984	0	0
	Cor (2,2)		1	1	1	1
	Cor (2,3)		0	1	0	0
	Cor (2,4)		0	0.9984	0	0
	Cor (2,5)		0	0.9984	0	0
Correlation coefficient	Cor (2,6)		0	0.9984	0	0
	Cor (3,3)		1	1	1	1
	Cor (3,4)		0	0.9984	0	0
	Cor (3,5)		0	0.9984	0	0
	Cor (3,6)		0	0.9984	0	0
	Cor (4,4)		1	1	1	1
	Cor (4,5)		0	0.9984	0	0
	Cor (4,6)		0	0.9984	0	0
	Cor (5,5)		1	1	1	1
	Cor (5,6)		0	0.9984	0	0
	Cor (6,6)		1	1	1	1

Table 4. Measured reaction cross-sections with uncertainty and correlation.

Type of reaction	E_n /MeV	Cross-section /Barns	Correlation matrix					
	13.83 ± 0.05	1.4189 ± 0.0694	1.0000					
^{127}I (n, 2n) ^{126}I	14.33 ± 0.10	1.5468 ± 0.0824	0.5893	1.0000				
	14.79 ± 0.10	1.5919 ± 0.0873	0.5892	0.5892	1.0000			
	13.83 ± 0.05	1.4836 ± 0.0719	0.5231	0.5231	0.5231	1.0000		
^{133}Cs (n, 2n) ^{132}Cs	14.33 ± 0.10	1.6402 ± 0.0878	0.5231	0.5231	0.5231	0.4658	1.0000	
	14.79 ± 0.10	1.8076 ± 0.1067	0.5231	0.5231	0.5231	0.4658	0.4658	1.0000

Cameron model (LEVDEN 0), while the transmission coefficients were calculated via the spherical optical model using ECIS-06 code with the global optical model potential, proposed by Koning and Delaroche for neutrons, taken from RIPL-3 library no. 204 [40, 41]. The statistical Hauser-Feshbach model was used to calculate the compound nucleus contribution [42]. For pre-equilibrium emission, the classical exciton model was used with the PCROSS code to calculate the pre-equilibrium contribution with a default mean free path multiplier (PCROSS 1.5).

V. RESULTS AND DISCUSSION

The cross-sections of the ^{127}I (*n, 2n*) ^{126}I and ^{133}Cs (*n, 2n*) ^{132}Cs reactions were determined relative to the monitor cross-section of ^{93}Nb (*n, 2n*) ^{92m}Nb at neutron energies of 13.83 ± 0.05, 14.33 ± 0.10, and 14.79 ± 0.10 MeV. The cross-sections with their uncertainties and correlation matrix are presented in Table 4. The final uncertainties of the ^{127}I (*n, 2n*) ^{126}I and ^{133}Cs (*n, 2n*) ^{132}Cs reaction cross-sections were 4.84%−5.90%. The measured cross-sections in this study are plotted in Figs. 3 and 5 along with the already existing experimental data reported in the EXFOR database. Moreover, the present results were compared with evaluated nuclear data from ENDF/B-VIII.0, JEFF-3.3, JENDL-5.0, BROND-3.1, CENDL-3.2, and TENDL-2021 and the nuclear reaction model codes EMPIRE-3.2.3 and TALYS-1.95.

A. ^{127}I (*n, 2n*) ^{126}I reaction

As shown in Fig. 3, the cross-sections of ^{127}I (*n, 2n*) ^{126}I were compared with the available literature data in the EXFOR database [2−15, 22]. The measurements in the approximately 14 MeV region exhibited a discrepancy between data measured by different groups, and the reported data by Qaim *et al*. and Martin *et al*. were lower than the data of this study and evaluated data [12, 15]. The cross-sections of this study were lower than data measured by Lin *et al*., Santry *et al*., and Maslov *et al*. but consistent with the evaluated data of the TENDL-2021 databases within the uncertainty range [3, 5, 6]. A considerable improvement in accuracy was achieved for the measured data in this study, which indicates that appropriate covariance analysis can improve data precision. Considering the correlation of uncertainties arising from various sources of experimental error, the final uncertainty results should be evaluated more accurately [33].

In addition, the excitation function of the ^{127}I (*n, 2n*) ^{126}I reaction was calculated theoretically using the TALYS-1.95 and EMPIRE-3.2.3 codes. As shown in Fig. 4, the theoretical cross sections calculated using TALYS-1.95 (ldmodels 1-6, preeqmode 1-4) and EMPIRE-3.2.3 were consistent with the present measured data, and the trend of the theoretical results was in accordance with the existing data. The excitation functions calculated by EMPIRE-3.2.3 were in good agreement with experimental data in shape and magnitude. However, the results measured by Santry *et al*. and Maslov *et al*. in the range 12-15 MeV and the evaluated data of the JEFF-3.3 and CENDL-3.2 databases at 9-20 MeV were higher than the excitation function calculated using the TALYS-1.95 and EMPIRE-3.3.2 codes [5, 6]. This shows that more experimental data are still needed to verify the accuracy of theoretical calculations.

B. Cross-section of the ^{133}Cs (*n, 2n*) ^{132}Cs reaction

The measured cross-sections of the reaction ^{133}Cs (*n, 2n*) ^{132}Cs are shown in Fig. 5 along with the existing data from the EXFOR database, in which the excitation functions of the ENDF/B-VIII.0, JEFF-3.3, and BROND-3.1 databases are exactly the same in shape and magnitude [6−8, 16−22]. The measurements in the approximately 14 MeV region exhibited a discrepancy between data meas-

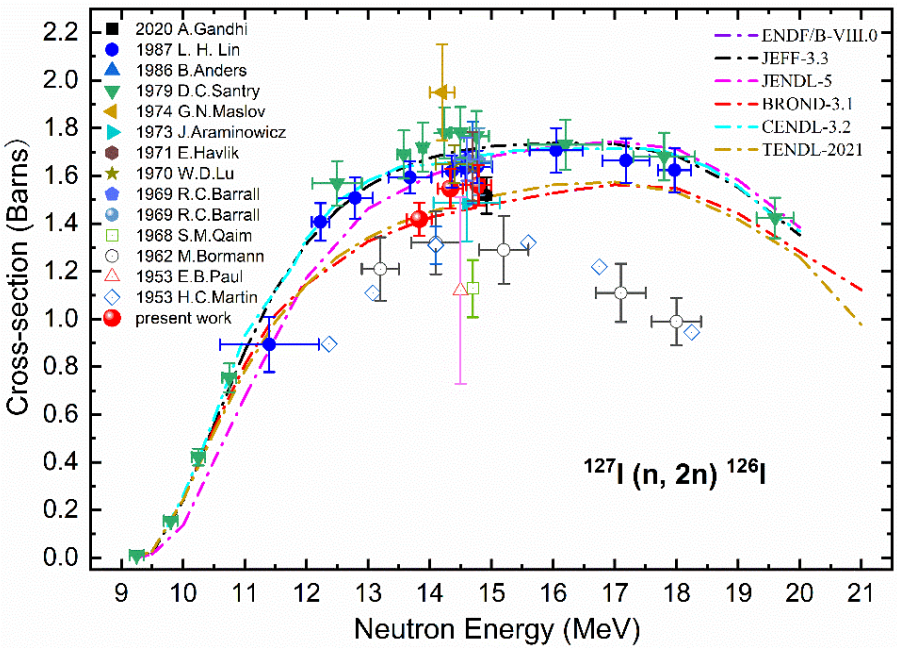

Fig. 3. (color online) Cross-section of the ^{127}I (*n, 2n*) ^{126}I reaction measured in this study and comparative studies with existing experimental cross-section data at different neutron energies and evaluated data.

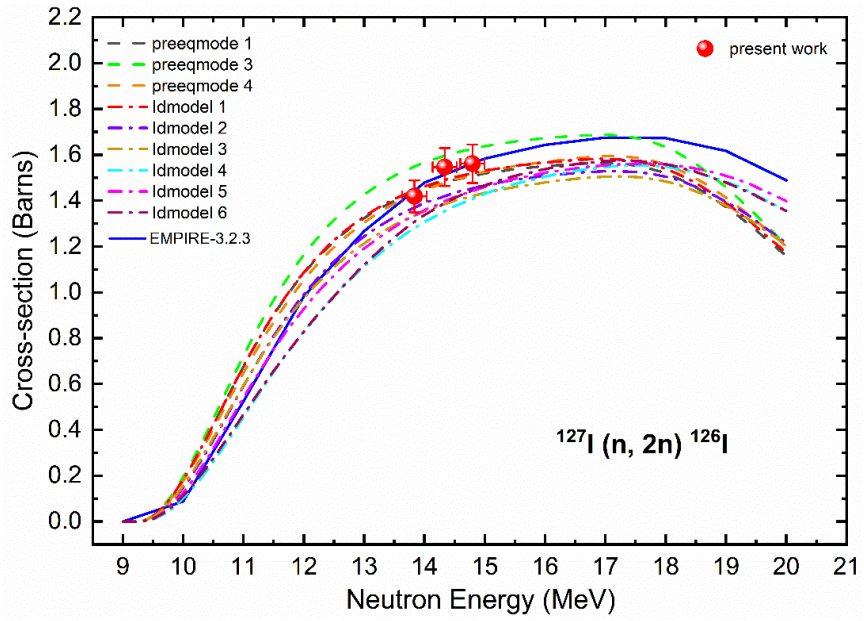

Fig. 4. (color online) Cross-section of the ^{127}I (n, 2n) ^{126}I reaction measured in this study and comparative studies with the theoretically calculated results from TALYS-1.95 (ldmodels 1-6, preeqmode 1-4) and EMPIRE-3.2.3.

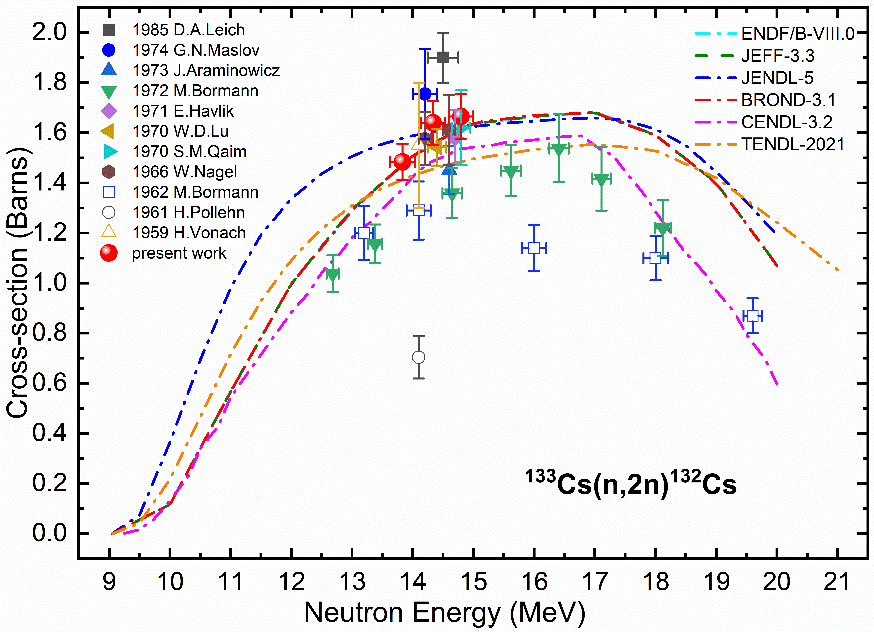

Fig. 5. (color online) Cross-section of the ^{133}Cs (n, 2n) ^{132}Cs reaction measured in this study and comparative studies with existing experimental cross-section data at different neutron energies and evaluated data.

ured by different groups. The cross-sections in this study were higher than data measured by Bormann *et al*. but consistent with the evaluated data of the ENDF/B-VIII.0, JEFF-3.3, and BROND-3.1 databases within the experimental uncertainties [13, 17].

The excitation function of the ^{133}Cs (n, 2n) ^{132}Cs reaction was calculated theoretically through the TALYS-1.95 and EMPIRE-3.2.3 codes. As shown in Fig. 6, the theoretically calculated results from the EMPIRE-3.2.3 and TALYS-1.95 (ldmodels 1-6, preeqmode 1-4) codes were also in good agreement with the present measurement at 14−17 MeV and followed the trend of experimental and evaluated data, which increased with increasing neutron energy at 10−17 MeV. The nuclear model using TALYS-1.95 code showed that the constant temperature and Fermi-gas model (ldmodel 1) was appropriate for

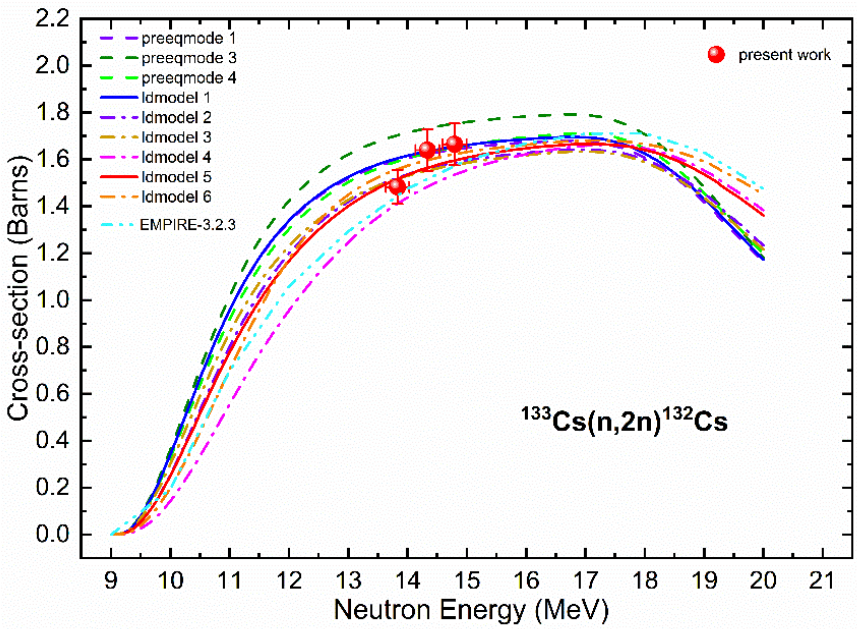

Fig. 6. (color online) Cross-section of the ^{133}Cs (n, $2n$) ^{132}Cs reaction measured in this study and comparative studies with the theoretically calculated results from TALYS-1.95 (ldmodels 1-6, preeqmode 1-4) and EMPIRE-3.2.3.

the cross-sections of the ^{133}Cs (*n, 2n*) ^{132}Cs reaction in the 14−15 MeV energy region, whereas that composed of microscopic level densities (Skyrme force) from Hilaire 's combinatorial tables (ldmodel 5) was consistent in the 13−14 MeV energy region. Furthermore, above 17 MeV, the evaluated data of the CENDL-3.2 databases were lower than other evaluated data and the excitation function calculated using the TALYS-1.95 and EMPIRE-3.3.2 codes. The excitation function calculated using the existing model was uniformly different from the evaluation database and experimental data. Therefore, more experimental data are still needed to verify the accuracy of theoretical calculations, and the theoretical calculation parameters must be further improved.

VI. CONCLUSIONS

In this study, the cross-sections of the ^{127}I (*n, 2n*) ^{126}I and ^{133}Cs (*n, 2n*) ^{132}Cs reactions induced by neutron energies of 13.83 ± 0.05, 14.33 ± 0.10, and 14.79 ± 0.10 MeV were measured relative to the reference reaction ^{93}Nb (*n, 2n*) ^{92m}Nb. The methodology of the covariance matrix was employed in the efficiency calibration of the HPGe detector and the uncertainty measurement of the ^{127}I (*n, 2n*) ^{126}I and ^{133}Cs (*n, 2n*) ^{132}Cs reaction cross-sections. The uncertainties in the measured cross-sections were in the range 4.84% ~ 5.90%, and the precision of the data was greatly improved compared with the available literature data in the EXFOR database. The present experimental results were in good agreement with the evaluated data from the ENDF/B-VIII.0, JEFF-3.3, BROND-3.1, and TENDL-2021 databases. In addition, the measured cross-sections were also reproduced using the theoretical nuclear reaction models EMPIRE-3.2.3 and TALYS-1.95. The excitation function calculated by EMPIRE-3.2.3 code was in good agreement with the experimental cross-sections of ^{127}I (*n, 2n*) ^{126}I in shape and magnitude. The excitation function calculated using the level density model of ldmodel 1 in TALYS-1.95 was consistent with experimental data in the 14−15 MeV energy region, while the excitation function calculated using ldmodel 5 was in good agreement with experimental data in the 13−14 MeV energy region. The accuracy of the current results, with detailed uncertainties and covariance information measured alongside the latest experimental data, was greatly improved, especially for the ^{133}Cs (*n, 2n*) ^{132}Cs reaction, providing covariance information for the first time. Accurate cross-section data contribute to improving the knowledge of cross-sections and optimizing the input parameters of models, which are critical for verifying nuclear reaction codes, particularly in the case of nuclear reactions with conflicting experimental data.

ACKNOWLEDGMENT

The authors are grateful to the staff of the K-400 Intense Neutron Generator at the China Academy of Engineering Physics for their excellent operation of the neutron generator and other support during the experiment.

References

[1] J. H. Luo *et al*., Eur. Phys. J. A **58**, 1 (2022)
[2] H. K. Gandhi *et al*., Phys. Rev. A **102**, 033528 (2020)
[3] H. Lu *et al*. , No. INDC (CPR)--16. International Atomic Energy Agency (1989)
[4] B. Anders *et al*., Radiat. Effects **92**, 211 (1986)
[5] D. Santry, Nuclear Cross Sections for Technology, 433 (1980).
[6] G. Maslov *et al*. , USSR report to the INDC, 10 (1974)
[7] J. Araminowicz and J. Dresler, NSA-29-006518 (1973)
[8] E. Havlik, Acta Phys. Austr. **34**, 209 (1971)
[9] W. D. Lu *et al*., Phys. Rev. C **1**, 350 (1970)
[10] R. C. Barrall *et al*. , STANFORD UNIV CA (1969)
[11] R. C. Barrall *et al*., Nucl. Phys. A **138**, 387 (1969)
[12] S. Qaim *et al*., J. Inorg. Nucl. Chem. **30**, 2577 (1968)
[13] M. Bormann, Z. Phys. **166**, 477 (1962)
[14] E. Paul *et al*., Can. J. Phys. **31**, 267 (1953)
[15] H. Martin *et al*., Phys. Rev. **89**, 1302 (1953)
[16] D. Leich *et al*. , Lunar and Planetary Science Conference, pp. 485. (1985)
[17] M. Bormann *et al*., Z. Phys. A **277**, 203 (1976)
[18] S. Qaim, J. Inorg. Nucl. Chem **32**, 1799 (1970)
[19] W. Nagel, No. NP-16748. Amsterdam Univ. (Netherlands, 1966)
[20] H. Pollehn and H. Neuert, Z. Naturforsch. A **16**, 227 (1961)
[21] H. Vonach, Oesterr. Akad. Wiss. Math-Naturw. Kl., Anzeiger **96**, 120 (1959)
[22] EXFOR. Database. https://www- nds.iaea.org/exfor/servlet/X4sSearch5
[23] A. Gandhi *et al*., Phys. Rev. C **102**, 014603 (2020)
[24] I. Pasha *et al*., Radiochim. Acta **108**, 679 (2020)
[25] S. Y. Sheela *et al*. , Internal report no. Mu/Stastics/DAE-BRNS/2017, 10.13140/RG. 2.2. 26729.49764 (2017)
[26] J. H. Luo *et al*., Nucl. Instrum. Methods. Phys. Res. Sect. B **298**, 61 (2013)
[27] C. L. Lan et al, J. Nucl. Sci. Technol. **60**, 251 (2023)
[28] V. Lewis and K. Zieba, Nucl. Instrum. Methods **174**, 141 (1980)
[29] J. Katakura and K. Kitao, Nucl. Data Sheets **97**, 765 (2002)
[30] Y. Khazov *et al*., Nucl. Data Sheets **104**, 497 (2005)
[31] C. M. Baglin *et al*., Nucl. Data Sheets **113**, 2187 (2012)
[32] A. W. Tyler *et al*., Phys. Rev. **56**, 125 (1939)
[33] B. Lawriniang *et al*., J. Radioanal. Nucl. Chem. **319**, 695 (2019)
[34] C. Lan *et al*., Nucl. Instrum. Methods. Phys. Res. Sect. B **525**, 18 (2022)
[35] G. Satchler, (Oxford Univ. Press, New York, 1983)
[36] J. Raynal, CEA Saclay report CEA-N-2772 (1994)
[37] C. Kalbach *et al*., Phys. Rev. C **33**, 818 (1986)
[38] P. Moldauer *et al*., Phys. Rev. C **14**, 764 (1976)
[39] P. Moldauer *et al*., Nucl. Phys. A **344**, 185 (1980)
[40] A. Koning and J. Delaroche, Nucl. Phys. A **713**, 231 (2003)
[41] R. Capote *et al*., Nucl. Data Sheets **110**, 3107 (2009)
[42] W. Hauser and H. Feshbach, Phys. Rev. **87**, 366 (1952)